Cancer Cell
Article

LZAP, a Putative Tumor Suppressor, Selectively Inhibits NF-κB

Jialiang Wang,[1,3] Hanbing An,[2,3] Marty W. Mayo,[5] Albert S. Baldwin,[6] and Wendell G. Yarbrough[1,2,3,4,*]
[1]Department of Cancer Biology
[2]Department of Otolaryngology
[3]Barry Baker Laboratory for Head and Neck Oncology
[4]Vanderbilt Ingram Cancer Center
Vanderbilt University, Nashville, TN 37232, USA
[5]Department of Biochemistry and Molecular Genetics, University of Virginia, Charlottesville, VA 22908, USA
[6]Department of Biology, University of North Carolina at Chapel Hill, Chapel Hill, NC 27599, USA
*Correspondence: wendell.yarbrough@vanderbilt.edu
DOI 10.1016/j.ccr.2007.07.002

SUMMARY

LZAP has been reported to inhibit cellular proliferation and clonogenic growth. Here, we report that decreased LZAP expression promoted cellular transformation, xenograft tumor growth, and xenograft tumor vascularity. Loss of LZAP also increased cellular invasion, and MMP-9 expression dependent on NF-κB. LZAP directly bound to RelA, impaired serine 536 phosphorylation of RelA, increased HDAC association with RelA, inhibited basal and stimulated NF-κB transcriptional activity, and was found at the promoter of selective NF-κB-responsive genes. LZAP protein levels were markedly decreased in 32% of primary HNSCCs (n = 28) and decreased LZAP levels in primary HNSCC correlated with increased expression of the NF-κB-regulated genes IL-8 and IκBα. In aggregate, these data support a role of LZAP in NF-κB regulation and tumor suppression.

INTRODUCTION

Tumor formation is a multistep process that involves activation of oncogenes and inhibition of tumor suppressors. At the cellular level, biologic activities of tumor suppressors frequently result in cell cycle arrest or apoptosis in response to oncogenic or mutagenic stimuli. On the other hand, activation of oncogenes is typically associated with cellular proliferation or protection from apoptosis. Oncogene and tumor suppressor activity must be tightly regulated to prevent uncontrolled proliferation and tumor formation, but also to avoid unnecessary cell death or proliferative arrest, either of which could harm the organism.

Proteins that simultaneously control activities of multiple tumor suppressors and/or oncogenes can drastically alter oncogenic potential. Some of the first examples of proteins capable of altering multiple tumor-related targets were discovered from oncogenic viruses. The simian virus 40 large T antigen inhibits tumor suppressors p53 and retinoblastoma (Rb) (Ahuja et al., 2005), and the human papilloma virus E6 protein inhibits p53 and Bax (Magal et al., 2005; Mantovani and Banks, 2001) but activates the human telomerase catalytic subunit (hTERT) (Liu et al., 2005). More recently, endogenous proteins have been found to regulate multiple proteins involved in tumorigenesis. MDM2, which inhibits and degrades p53, can also inhibit and mediate degradation of Rb (Ying and Xiao, 2006). Likewise, the ARF tumor suppressor ($p14^{ARF}$ in human, $p19^{ARF}$ in mouse) simultaneously activates p53 and inhibits the transcriptional activity of nuclear factor-κB (NF-κB) (Rocha et al., 2003; Zhang et al., 1998). NF-κB is a family of pluripotent transcription factors that play a fundamental role in inflammatory and immune responses as well as tumorigenesis. All NF-κB proteins

SIGNIFICANCE

NF-κB is activated in a wide range of human cancers, including head and neck squamous cell carcinoma, and has been implicated in tumor progression at least partially through promotion of invasion and angiogenesis and by inhibition of apoptosis. Recently, tumor suppressors such as ARF and CYLD have been shown to inhibit NF-κB, contributing to their antitumor activities. Using both in vivo and in vitro assays, we show that LZAP potently inhibits NF-κB and has tumor suppressor-like activity. Loss of LZAP was found in one-third of primary head and neck squamous cell carcinomas and correlated with increased expression of the NF-κB-regulated genes IL-8 and IκBα. Loss of LZAP may represent a distinct mechanism leading to increased NF-κB activity in human tumors.

contain Rel homology domains that mediate DNA binding, dimerization, and nuclear localization. Active NF-κB requires dimerization of two subunits. The heterodimer of RelA/p50 is the most intensely studied form of NF-κB complex, and many oncogenic activities such as stimulation of proliferation, angiogenesis, invasion, transformation, and inhibition of apoptosis have been attributed to it (Karin et al., 2002). NF-κB activity is tightly and intricately controlled, most notably through binding IκB proteins that tether NF-κB in the cytoplasm until nuclear translocation is induced by signal-initiated IκB degradation (Hayden and Ghosh, 2004). It has recently been recognized that nuclear localization alone is insufficient to fully activate NF-κB transcription. Nuclear events including posttranslational modification and association with transcriptional coactivators are necessary for full NF-κB activation (Chen and Greene, 2004). Association with transcriptional corepressors can inhibit NF-κB transcription despite nuclear localization. The discovery of nuclear regulatory events suggests that NF-κB activity is not only defined by mass translocation from the cytoplasm to the nucleus.

We previously described that LZAP activates the tumor suppressor p53 and inhibits clonogenic growth of tumor cell lines in vitro (Wang et al., 2006). LZAP has also been found to promote apoptosis in response to genotoxic agents such as etoposide through regulation of the Cdk1-cyclinB1 complex (Jiang et al., 2005). Here, we describe additional LZAP activity as an inhibitor of NF-κB independent of ARF or p53. Depletion of LZAP increased cellular invasion and MMP-9 expression both of which were dependent on NF-κB and was associated with in vitro cellular transformation. In vivo studies revealed that diminished LZAP levels enhanced xenograft tumor growth and angiogenesis. Loss of LZAP protein was observed in approximately 30% of human head and neck squamous cell carcinomas (HNSCC), and in these tumors, LZAP expression inversely correlated with expression of a subset of NF-κB target genes.

RESULTS

LZAP Protein Levels Are Dramatically Decreased in a Portion of Human Head and Neck Squamous Cell Carcinomas

We identified LZAP as an ARF-binding protein that activates p53 in ARF-dependent and -independent manners. Expression of LZAP reduces cellular proliferation and clonogenic growth of p53-positive cells (Wang et al., 2006), and loss of LZAP protects HeLa cells from apoptosis induced by genotoxic agents such as etoposide or X-ray irradiation through regulation of Cdk1-cyclinB1 (Jiang et al., 2005). These observations led us to explore a potential tumor suppressor role for LZAP. Since many tumor suppressors are inactivated in tumors through loss of expression, we examined LZAP protein levels in tumors and histologically normal epithelium adjacent to tumor (NAT) from head and neck squamous cell carcinoma (HNSCC) patients (n = 28, 17 incident and 11 recurrent tumors). Frozen tumor and NAT were macrodissected with histological guidance to ensure that the tumor and normal adjacent tissue samples contained at least 70% epithelial cells. LZAP levels within cancer tissue and the normal adjacent epithelium were determined by quantification of band intensity after immunoblotting and normalization to GAPDH as a loading control. Mean LZAP levels observed in HNSCCs were lower than those observed in normal surrounding epithelia, but the mean levels differed by less than 2-fold (Figure 1A). However, while LZAP expression in the normal epithelia adjacent to tumors clustered in a single group around the mean, HNSCCs could be separated into three groups based on LZAP expression. LZAP levels in the majority of tumors (19 of 28) clustered in a pattern around a mean similar to the mean and pattern observed in NAT (similar to NAT group). Nine of 28 (32%) HNSCC had lower LZAP expression, and these tumors were divided into subgroups based on LZAP expression. By immunoblotting, five tumors lacked detectable bands at the molecular weight of LZAP (undetectable LZAP group), while another four tumors had faint LZAP bands (trace LZAP group) by immunoblotting. Pairwise comparison between individual HNSCC and NAT derived from the same patient revealed that LZAP expression in tumors was reduced by more than 50% in 15 of 28 tumors (54%). Conversely, 4 of 28 tumors contained LZAP protein levels that were elevated by more than 2-fold compared with NAT. The remaining nine HNSCCs had LZAP levels similar to matched NAT.

Depletion of LZAP Induces Primary Cell Transformation In Vitro

LZAP protein was markedly decreased in a portion of primary human HNSCCs, suggesting that LZAP may have a role in prevention of tumor formation. To determine if endogenous LZAP protected against cellular transformation, anchorage-independent growth was measured after LZAP expression was inhibited by retrovirally delivered shRNA in immortalized but not transformed TLM-HMEC cells (Westbrook et al., 2005). Compared to cells infected with control retrovirus, cells lacking LZAP had an approximate 9-fold increase in colony number and produced larger colonies (Figure 1B). Loss of LZAP expression was confirmed in a portion of the cells prior to soft agar plating (Figure 1B). Since p53 is inactivated in TLM-HMEC cells by large T antigen, increased soft agar growth associated with LZAP loss was attributable to p53-independent activities.

Decreased LZAP Expression Promotes Xenograft Tumor Formation

To further explore a potential role of LZAP as a tumor suppressor, nude mice xenografts were modeled using HeLa cells following inhibition of LZAP expression by retrovirally delivered shRNA. HeLa cells were chosen because they reliably form tumors in nude mice, but not in 100% of inoculated sites, thereby enabling measurements of tumor incidence as well as tumor growth. Additionally, HeLa cells lack p53 activity, so LZAP-mediated effects on tumor development could be attributed

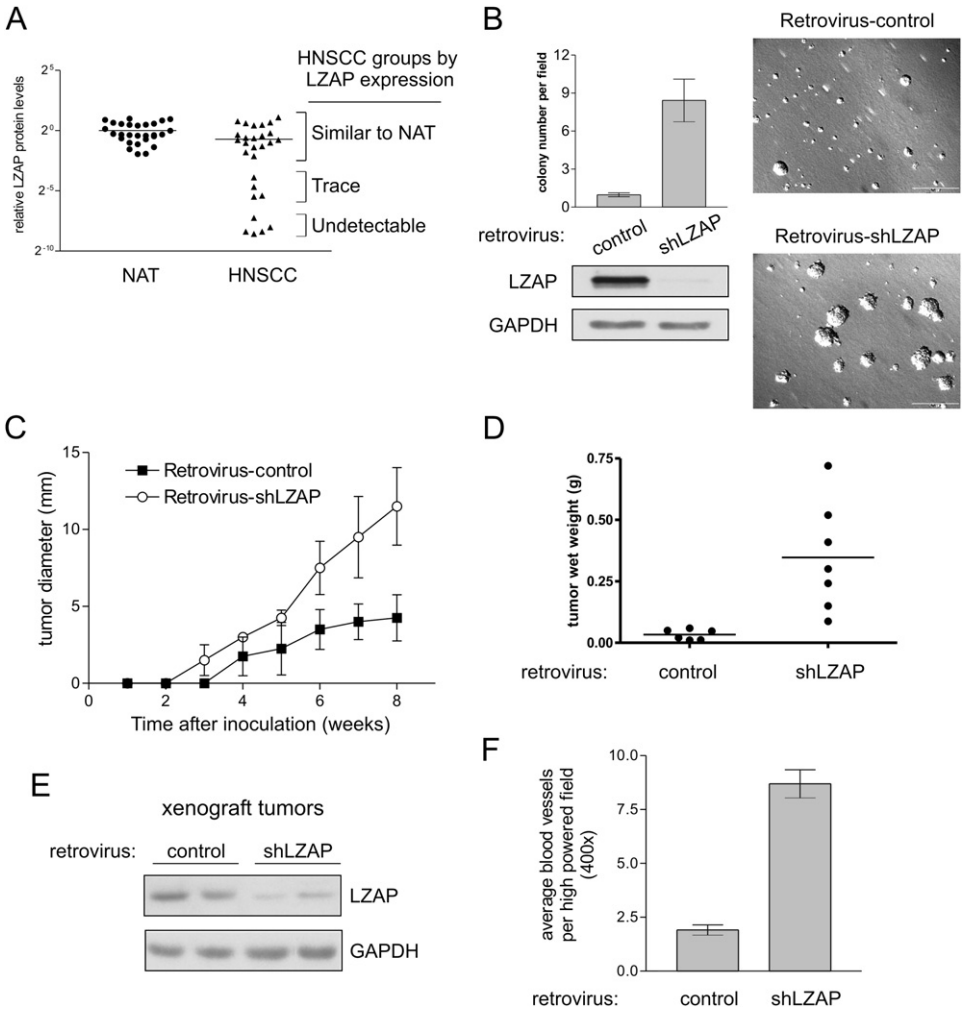

Figure 1. LZAP Has Tumor Suppressor-like Qualities

(A) LZAP is downregulated in human head and neck squamous cell carcinomas (HNSCC). Relative LZAP expression was determined by immunoblotting lysate from 28 pairs of frozen HNSCCs and surrounding normal epithelia adjacent to tumor (NAT). LZAP levels were corrected for loading based on expression of GAPDH. Mean LZAP level in NAT was set as 1. Three groups of HNSCC based on LZAP expression are defined.

(B) Depletion of LZAP expression promotes cellular transformation. TLM-HMEC cells were infected with control retrovirus or retrovirus encoding shRNA specific to LZAP, selected by puromycin, and plated into soft agar. Colonies were counted 2 weeks after initial plating. Data were generated from two independent experiments, each in triplicate (error bars = mean ± SD). For each experiment, ten low-powered fields (100×) were counted per well. Loss of LZAP expression in cells prior to plating was confirmed by immunoblotting. Representative photomicrographs of TLM-HMEC colonies are shown (scale bars, 200 μm).

(C) Decreased LZAP levels enhance xenograft tumor growth. HeLa cells were infected with either control retrovirus or retrovirus delivering LZAP-specific shRNA and selected with puromycin. Three mice (six injections) were inoculated with control HeLa cells and three with LZAP knockdown cells. Tumor growth was monitored weekly by measurement of diameter until the largest tumor diameter approached 15 mm (error bars, mean ± SD).

(D) HeLa xenografts with diminished LZAP expression were larger than control xenografts. Tumors from two independent xenograft experiments were weighed immediately after removal. Mean xenograft tumor weight is indicated.

(E) Immunoblotting of LZAP in representative xenograft tumors at the time of sacrifice. Two control and two LZAP knockdown HeLa xenograft tumors from the experiment described in Figure 1A. Tumors were macrodissected to enrich for epithelial tumor cells prior to immunoblotting.

(F) Loss of LZAP in xenograft tumors is associated with increased blood vessel density. Five micrometer sections of xenograft tumors described in Figure 1C were immunostained with von Willebrand Factor (vWF)-specific antibodies. Mean number of vWF-positive vessels per high-powered field (400×) and standard error are presented. Results represent vessel density determined from at least six independent high-powered fields per tumor.

to p53-independent activities of LZAP. For each of two independent experiments, six nude mice were divided into two equal groups and inoculated with either control cells or LZAP knockdown cells into both flanks. Comparison of the average tumor latency and diameter revealed that LZAP knockdown tumors emerged earlier and proliferated to a greater size compared to control tumors (Figure 1C). At the end of the experimental period, the final wet weights of LZAP knockdown tumors were found to be markedly higher than control tumors

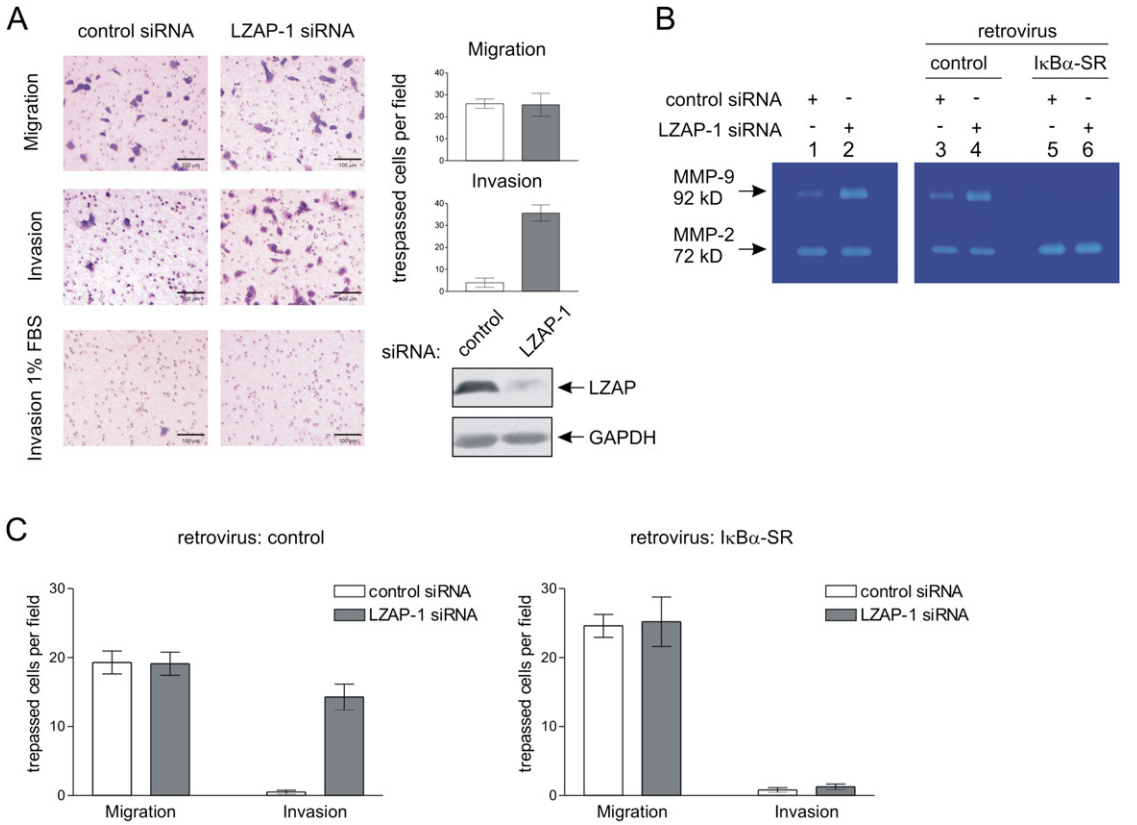

Figure 2. Decreased LZAP Expression Enhances NF-κB-Dependent Cell Invasion and MMP-9 Expression

(A) Depletion of LZAP promotes cell invasion. U2OS cells were transfected with siRNA as indicated. Migration or invasion through transwells without or with matrigel, respectively, was measured by direct counting of trespassed cells. Representative photomicrographs are shown (scale bars, 100 μm). Results represent cell counts from at least five randomly selected low-powered fields (200×) from three independent experiments (error bars, mean ± SEM). Media containing 1% FBS in the lower chamber served as control. Immunoblotting was used to confirm LZAP expression before seeding of cell into transwells.

(B) LZAP knockdown increases MMP-9 expression. Levels of MMP-2 and MMP-9 in conditioned medium derived from siRNA-transfected U2OS cells were determined by gelatin-based zymography (lanes 1 and 2). Similar zymography was performed after infection with control or mutated IκBα-super-repressor (IκBα-SR) expressing retroviruses as indicated (lanes 4–6).

(C) Matrigel invasion is dependent on NF-κB activity. Migration and invasion assays following transfection of siRNA as indicated were performed in U2OS cells infected with control or IκBα-SR-encoding retrovirus. Migration and invasion were measured as described above (error bars, mean ± SEM).

(Figure 1D). Although tumor latency and tumor size were altered by loss of LZAP expression, tumor incidence was similar in this xenograft model (6/12 control, 7/12 LZAP knockdown). Immunoblotting of LZAP in representative xenograft tumors indicated that diminished LZAP expression had been maintained throughout the experimental time course (Figure 1E).

Upon harvesting of xenograft tumors at the completion of the experiments, gross inspection of the tumors revealed that LZAP knockdown tumors were pink, whereas control tumors were white, suggesting that vascularity may differ. To determine blood vessel density within tumors, immunohistochemical staining of von Willebrand Factor (vWF) followed by direct counting of blood vessels in nonnecrotic tumor regions was performed. Blood vessel density was increased roughly 4-fold in LZAP knockdown tumors relative to control tumors (Figure 1F). Lungs of mice bearing xenograft tumors were examined but revealed no metastases in either control or LZAP knockdown groups (data not shown).

Depletion of Endogenous LZAP Induces NF-κB-Dependent MMP-9 Expression and Cell Invasion In Vitro

To provide further insight into tumor-related activities of LZAP, in vitro cell invasion through a matrigel barrier was measured after LZAP expression was decreased. Invasion was infrequent in control U2OS cells and absent without serum as an attractant; however, following siRNA-mediated inhibition of LZAP expression, invasion was increased approximately 9-fold (Figure 2A). Diminished LZAP expression did not alter cellular migration through the transwells in the absence of matrigel (Figure 2A). Reduction of endogenous LZAP proteins levels following transient transfection of siRNA was confirmed by immunoblotting (Figure 2A).

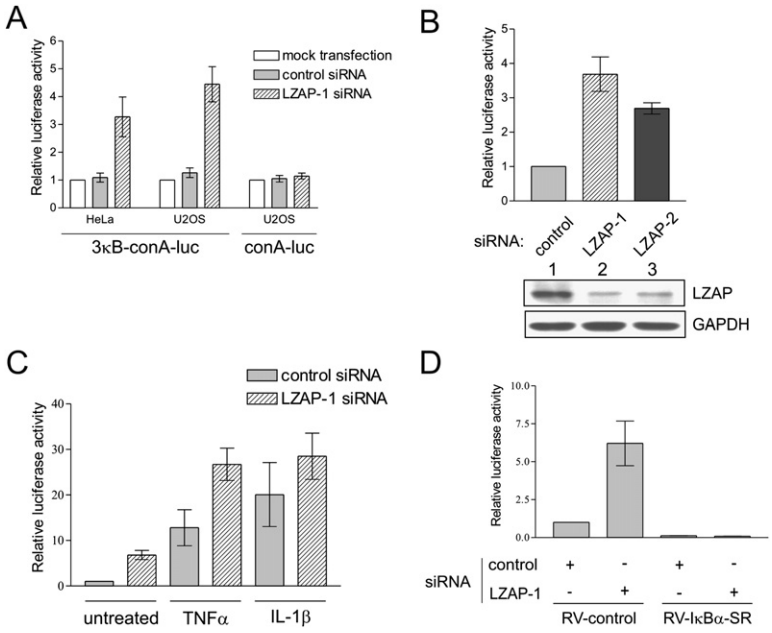

Figure 3. Decreased LZAP Expression Activates NF-κB-Mediated Transcription

(A) Depletion of LZAP increased basal NF-κB activity. HeLa or U2OS cells were transiently transfected with control siRNA or siRNA specific to LZAP (LZAP-1) along with a control (conA-luc) or NF-κB-responsive (3κB-conA-luc) luciferase reporter as indicated. Luciferase activities were determined by the dual luciferase assay system 2 days after transfection. In this and subsequent luciferase assays, firefly luciferase activity was normalized to coexpressed *renilla* luciferase from the CMV promoter as the internal control, and normalized firefly luciferase activity from cells transfected with control reagents was assigned a value of 1. All luciferase assay data are expressed as the mean ± standard error of at least three independent experiments.

(B) Two distinct LZAP siRNAs (LZAP-1 and LZAP-2) reduce LZAP expression and increase NF-κB transcriptional activity. Luciferase NF-κB reporter assays were performed after transfection of U2OS cells with indicated siRNA constructs. LZAP levels were confirmed by immunoblotting.

(C) Decreased LZAP expression potentiates TNFα or IL-1β activation of NF-κB. U2OS cells were transfected with siRNA constructs as indicated before luciferase assay. Untreated cells or cells treated with 10 ng/ml TNFα or 2 ng/ml IL-1β were assayed for NF-κB-dependent luciferase activity.

(D) Luciferase activity induced by depletion of LZAP is NF-κB dependent. Transfection of siRNA constructs and subsequent luciferase assays were performed in U2OS cells infected with control or IκBα-SR-encoding retrovirus.

Matrix metalloproteinases (MMPs) comprise a family of secreted or membrane-associated zinc-dependent extracellular endopeptidases that enhance invasion and metastases (Fingleton, 2006). To determine if increased invasion observed with loss of LZAP expression was associated with concomitant change of matrix metalloproteinase levels, gelatin-based zymography assays measuring expression of MMP-2 and MMP-9 were performed. MMP-9 levels were increased following LZAP knockdown, whereas MMP-2 levels were not altered by loss of LZAP (Figure 2B, lanes 1 and 2). NF-κB regulates MMP-9 and/or MMP-2 expression in various cells (Bond et al., 1998; He, 1996; Kim and Koh, 2000; Takada et al., 2005). To determine if increased MMP-9 expression observed in U2OS cells following loss of LZAP expression was dependent on NF-κB, zymography assays were repeated in cells stably expressing a degradation-resistant mutant of the NF-κB inhibitor IκBα (IκBα-super-repressor [IκBα-SR]). MMP-9 activity was undetectable in the presence of IκBα-SR regardless of LZAP status, suggesting that NF-κB activity was required for basal and LZAP-regulated MMP-9 expression (Figure 2B, lanes 3–6). Similarly, constitutive expression of MMP-9, as well as elevated expression associated with LZAP loss, was partially abrogated by simultaneous siRNA-mediated repression of RelA expression (Figure S1A in the Supplemental Data available with this article online). MMP-2 activity was not altered by expression of IκBα-SR, indicating that NF-κB was dispensable for basal MMP-2 expression in U2OS cells. Additionally, matrigel invasion assays in the presence of IκBα-SR or knockdown of RelA revealed that the invasive phenotype caused by loss of LZAP was also dependent on NF-κB activity (Figure 2C and Figure S1B).

Depletion of Endogenous LZAP Activates NF-κB

LZAP knockdown was associated with increased NF-κB-dependent expression of MMP-9 (Figure 2B). To further elucidate the effect of LZAP on NF-κB transcriptional activity, luciferase reporter assays with an NF-κB-responsive promoter (3κB-conA-luc) were performed in U2OS and HeLa cells following treatment with LZAP-specific siRNA. Depletion of LZAP resulted in a significant increase of NF-κB activity relative to mock or control siRNA-transfected cells (Figure 3A). In contrast, luciferase expression from the conA-luc control reporter, which is not responsive to NF-κB, was not altered by depletion of LZAP (Figure 3A and data not shown). To exclude the possibility that off-target effects of siRNA were responsible for activation of NF-κB, results were confirmed using an alternative siRNA targeting an independent LZAP sequence (LZAP-2) (Figure 3B).

Cytokines such as TNFα or IL-1β rapidly and potently activate NF-κB transcription. To determine if endogenous LZAP regulated cytokine-induced NF-κB activation, NF-κB activity was determined in TNFα- or IL-1β-treated cells after siRNA-directed loss of LZAP. Loss of LZAP was associated with further enhancement of NF-κB activity following cytokine stimulation (Figure 3C).

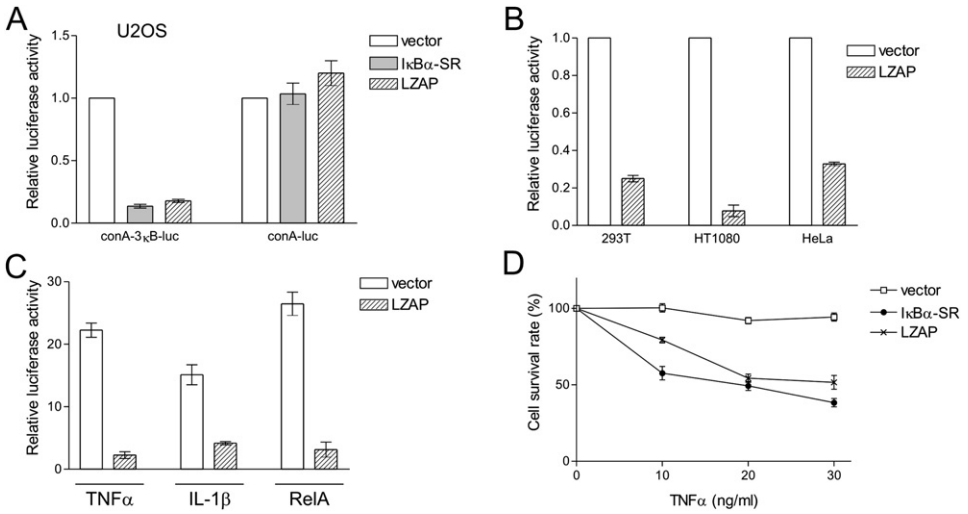

Figure 4. Overexpression of LZAP Inhibits NF-κB Transcriptional Activity

(A) LZAP inhibits NF-κB transcriptional activity. U2OS cells were transfected with plasmids encoding LZAP or IκBα-SR in addition to the NF-κB-responsive reporter 3κB-conA-luc or the NF-κB-independent reporter conA-luc, as indicated. Two days after transfection, luciferase activities were determined as described in Figure 3A.

(B) Expression of LZAP inhibits NF-κB transcriptional activity in 293T, HT1080, and HeLa cells. Luciferase reporter assays using the 3κB-conA-luc reporter were performed in the three cell lines after transfection with control or LZAP plasmids as indicated.

(C) LZAP blocks NF-κB activation by cytokines or expression of RelA. Luciferase reporter assays were performed in U2OS cells following 4 hr TNFα or IL-1β treatment with or without LZAP expression. Alternatively, 10 ng pcDNA3-Myc-RelA was cotransfected with 1 μg empty vector or DNA construct encoding LZAP prior to luciferase reporter assays.

(D) LZAP sensitizes HT1080 cells to TNFα-induced apoptosis. HT1080 cells were transfected as indicated followed by puromycin selection and treatment with indicated doses of TNFα for 24 hr. Cells were stained with trypan blue, and live cells were counted. Data presented are the mean ± standard error generated from three independent experiments.

To confirm that the reporter activity measured from the 3κB-conA-Luc construct was dependent on NF-κB activity, U2OS cells were infected with retrovirus directing expression of IκBα-SR before measuring NF-κB activity. As expected, luciferase activity was nearly undetectable in cells stably expressing IκBα-SR regardless of LZAP status (Figure 3D). Additionally, enhancement of NF-κB activity seen with LZAP knockdown was partially inhibited with simultaneous knockdown of RelA (Figure S1C). Collectively, these results suggest that endogenous LZAP repressed both basal and cytokine-induced NF-κB activity.

LZAP Inhibits NF-κB Transcriptional Activity

To further explore the role of LZAP in regulation of NF-κB, reporter assays were performed following expression of LZAP. In U2OS cells, ectopic expression of LZAP inhibited basal NF-κB transcription to a similar degree as the well-characterized IκBα-SR (Figure 4A). Luciferase expression from the control reporter (conA-luc) was not altered by LZAP or IκBα-SR expression (Figure 4A). Our previous study indicates that LZAP affects ARF and p53 activities, both of which have been reported as NF-κB inhibitors. To determine if LZAP activity toward NF-κB required either ARF or p53, luciferase reporter assays were repeated in HT1080 (human fibrosarcoma, ARF negative, p53 wild-type), HeLa (human cervical adenocarcinoma, containing human papilloma virus type 18 E6 and E7 proteins), and 293T (human kidney epithelial cells expressing adenoviral E1A and E1B proteins and SV40 large T antigen) cells. In all three cell lines, expression of LZAP reduced basal NF-κB activity regardless of ARF or p53 status (Figure 4B). Inhibition of NF-κB transcriptional activity was confirmed using a different NF-κB-dependent luciferase reporter (p65-luc; data not shown). Additionally, luciferase reporter assays following TNFα or IL-1β treatment demonstrated that NF-κB activity induced by cytokines was markedly decreased in cells expressing LZAP (Figure 4C). Similar results were observed in three additional cell lines examined (293T, HeLa, and HT1080; data not shown). Expression of LZAP also inhibited NF-κB activity associated with ectopic expression of RelA (Figure 4C).

LZAP Sensitizes HT1080 Cells to TNFα-Induced Cell Death

Constitutive NF-κB activation within many human tumor types promotes tumor survival following administration of chemotherapeutic agents or in response to cytokine stimulation. TNFα activates apoptotic pathways but rarely results in massive cell death due to simultaneous induction of NF-κB; however, inhibition of NF-κB sensitizes the chemoresistant HT1080 cells to TNFα-induced apoptosis (Wang et al., 1996). To determine if expression of LZAP similarly increased cytokine-induced apoptosis, HT1080 cell survival was evaluated after treatment with increasing concentrations of TNFα. Like IκBα-SR,

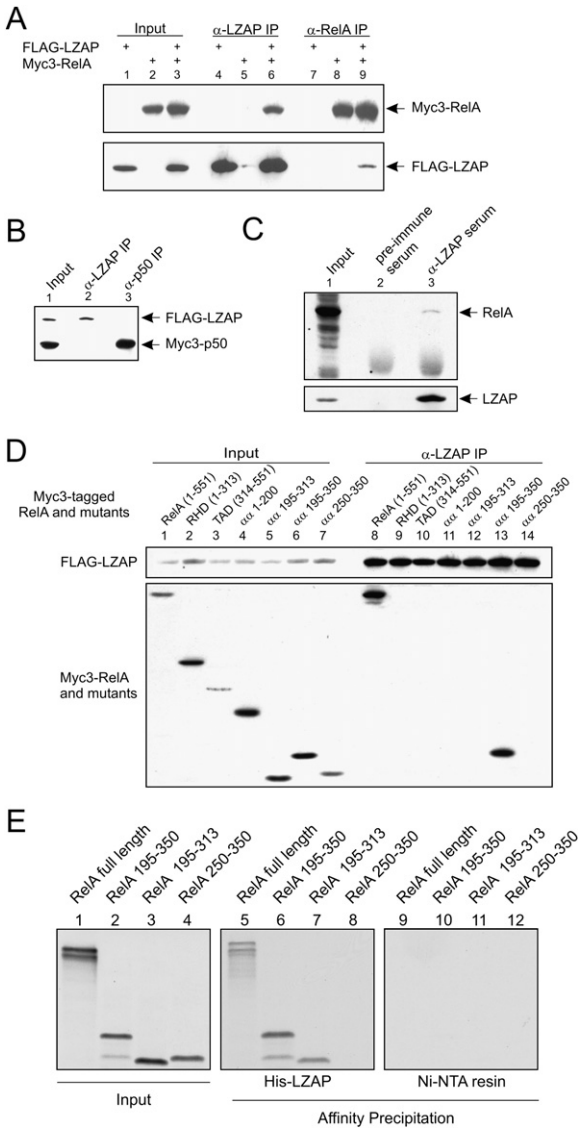

Figure 5. LZAP Directly Interacts with RelA

(A) Ectopically expressed LZAP and RelA mutually coimmunoprecipitate. U2OS cells were transfected with indicated plasmids directing expression of tagged LZAP or RelA. Immunoprecipitates were prepared using rabbit antibodies recognizing LZAP or RelA, resolved on SDS-PAGE, and immunoblotted by HRP-conjugated Myc or FLAG antibodies. In this and subsequent immunoprecipitation experiments, 5% of each input lysate was loaded as reference (input).

(B) LZAP does not bind to p50. U2OS cells were transfected with plasmids directing expression of LZAP and p50, and lysate was immunoprecipitated using LZAP- or p50-specific antibodies, then immunoblotted with HRP-conjugated antibodies specific to Myc or Flag.

(C) Endogenous LZAP binds endogenous RelA. Lysates from untransfected 293T cells were immunoprecipitated with preimmune or LZAP-specific rabbit antiserum, then immunoblotted with antibodies specific to RelA and LZAP.

(D) Extended C-terminal portion of the Rel homology domain of RelA is sufficient for LZAP interaction. Myc3-tagged truncation mutants of RelA were coexpressed in U2OS cells with full-length LZAP. LZAP was immunoprecipitated, and RelA mutants were identified by Myc immunoblotting.

expression of LZAP resulted in a dose-dependent loss of cell viability in response to TNFα (Figure 4D).

LZAP Directly Binds to RelA

To begin exploring mechanisms by which LZAP inhibited NF-κB, LZAP binding to NF-κB proteins was tested in mammalian cells by coimmunoprecipitation of transiently expressed FLAG-tagged LZAP and/or Myc-tagged RelA. When coexpressed, LZAP was readily detected from RelA immunoprecipitates and RelA was reciprocally co-precipitated using LZAP antibody (Figure 5A). These data suggest that only a portion of LZAP and RelA within cells interact. Antibody crossreaction was not detected from cells singly expressing either LZAP or RelA. In contrast, coimmunoprecipitation of overexpressed LZAP and p50 yielded no detectable interaction (Figure 5B). RelA was detected in immunoprecipitates prepared from untransfected 293T cells using an anti-LZAP serum but not in precipitates using a preimmune rabbit serum (Figure 5C); however, LZAP could not be detected in the reciprocal immunoprecipitation using RelA-specific antibody (data not shown).

To define the region of RelA protein required for LZAP interaction, immunoprecipitation experiments were performed using a series of RelA truncation mutants. Neither the Rel homology domain (RHD, aa 1–313) nor the transcription activation domain (TAD, aa 314–551) efficiently bound to LZAP (Figure 5D). Further screening showed that an extended amino-terminal region of RelA (aa 1–350) including the RHD domain was sufficient for LZAP binding (data not shown). Within this region, the DNA-binding domain (aa 1–200) was unable to interact with LZAP, whereas amino acid residues 195–350 strongly interacted with LZAP (Figure 5D, lane 13). Further deletion of this region, either at the amino (leaving aa 250–350) or carboxyl (leaving aa 195–313) terminus, abolished the robust interaction. Longer exposure allowed detection of aa 195–313 of RelA, but not aa 250–350, associated with LZAP (Figure 5D and data not shown).

Detection of RelA within LZAP immunoprecipitates from cell lysates could represent direct or indirect LZAP-RelA binding. To begin to distinguish these possibilities, we used bacterially expressed histidine-tagged LZAP to pull down full-length or truncation mutants of RelA generated through cell-free in vitro transcription and translation. Consistent with in vivo experiments, LZAP interacted with full-length RelA, and RelA truncation mutants containing aa 195–313 and aa 195–350, but not with aa 250–350 (Figure 5E, lanes 5–8). All RelA peptides were expressed well, and nickel beads without histidine-tagged

(E) LZAP binds to RelA in vitro. Myc-tagged full-length RelA and RelA truncation mutants were synthesized by in vitro transcription/translation in the presence of ^{35}S-methionine before incubation with bacterially expressed His6-tagged LZAP. Protein complexes bound to Ni-NTA resin were separated by gel electrophoresis and visualized by autoradiography. Ni-NTA resin was used as negative control. Input corresponds to 10% of IVT proteins used for pulldown assays.

LZAP did not associate with any RelA peptide. The minimal region tested capable of binding LZAP included aa 195–313; however, in vivo data suggested that extension of RelA truncation mutant to include aa 195–350 allowed more robust interaction with LZAP.

LZAP Does Not Interfere with Nuclear Translocation or DNA Binding of RelA

NF-κB activity is regulated in both the cytoplasm and nucleus. Cytoplasmic events, including sequential phosphorylation, polyubiquitination, and degradation of IκB proteins, result in NF-κB nuclear translocation. To determine if inhibition of NF-κB activity observed with expression of LZAP was associated with inhibition of RelA nuclear translocation, subcellular localization of RelA was determined following TNFα stimulation in cells expressing ectopic LZAP. In cells without TNFα stimulation, RelA protein was predominately cytoplasmic regardless of the expression status of LZAP. TNFα treatment triggered RelA nuclear accumulation in both LZAP-expressing and control cells (Figure S2A). Immunofluorescent staining of RelA in cells transfected with LZAP-1 siRNA showed no detectable difference in cytoplasmic RelA compared to control cells (Figure S2B). Reduction of endogenous LZAP expression and increase of NF-κB activity were confirmed in parallel experiments (data not shown).

DNA-binding activity of NF-κB in the presence or absence of LZAP was determined using an ELISA-based DNA-binding assay following TNFα stimulation. DNA-bound RelA subunits were identified using specific antibodies and visualized by chemiluminescence. As expected, nuclear extracts prepared from U2OS cells expressing ectopic IκBα-SR contained less RelA capable of binding DNA at all time points after TNFα stimulation. Expression of LZAP did not significantly alter DNA-binding activity of RelA at any time point (Figure S2C). Consistent with DNA binding and RelA cellular localization studies, TNFα-induced IκBα phosphorylation and IκBα protein degradation over a time course was not significantly altered by LZAP expression (Figure S2D) Collectively, our data suggest that inhibition of NF-κB by LZAP does not rely on altering IκBα degradation, RelA nuclear translocation, or RelA DNA binding.

LZAP Impairs Phosphorylation of RelA at Serine 536

Phosphorylation of RelA protein is required for its full activation. Among the several known phosphorylation sites of RelA, serine residues 276, 529, and 536 modified by a variety of kinases have been shown to increase DNA binding and/or transactivation (Viatour et al., 2005). To determine the effect of LZAP on RelA phosphorylation, Myc-tagged RelA was transiently expressed in U2OS cells with or without LZAP. Following TNFα stimulation, RelA protein was precipitated before immunoblotting with RelA phosphoserine-specific antibodies. Phosphorylation at serine 536 of RelA was decreased in LZAP-expressing cells, while phosphorylation at serines 276 and 529 were not altered (Figure 6A). The effect of loss of LZAP expression on phosphorylation of RelA serine 536 was confirmed by direct immunoblotting following transient transfection of the LZAP-1 siRNA. Loss of LZAP expression correlated with increased phosphorylation at serine 536 of RelA either with or without IL-1β or TNFα stimulation (Figure 6B).

We next compared the effect of LZAP on the transactivation of fusion proteins comprising the amino-terminal Gal4 DNA-binding domain and carboxyl-terminal full-length RelA (Gal4-RelA) or RelA with an activation mutation at serine 536 (Gal4-RelAS536D) designed to mimic phosphorylation at this site. Expression of LZAP inhibited transcription mediated by Gal4-fused wild-type RelA to a greater extent than Gal4-RelAS536D (Figure 6C). These data indicate that LZAP inhibition of RelA is partially dependent on its ability to alter phosphorylation of serine 536.

LZAP Enhances RelA Association with HDAC1, HDAC2, and HDAC3

Recent studies have demonstrated that UV-C, doxorubicin, and the tumor suppressor ARF can inhibit NF-κB activity by increasing RelA association with histone deacetylases (HDACs) and conversion of NF-κB into an active transcription repressor (Perkins, 2004). To determine if a similar mechanism contributed to inhibition of NF- κB by LZAP, HDAC complexes were precipitated from cells expressing Myc-tagged RelA with or without LZAP and immunoblotted for RelA. In LZAP-expressing cells, more RelA protein was associated with HDAC1, HDAC2, and HDAC3 (Figure 6D).

LZAP Regulates Expression of a Subset of NF-κB-Responsive Genes

To determine which NF-κB-responsive genes were regulated by LZAP, expression of 15 NF-κB-regulated genes was evaluated in siRNA-transfected U2OS cells using quantitative reverse transcription PCR (qRT-PCR, TaqMan gene expression assay, ABI). Six of the fifteen genes were increased less than 2-fold following TNFα stimulation, confirming that NF-κB regulation of these genes is cell type specific (Table S1). Among the nine genes that were responsive to TNFα, loss of LZAP increased expression of IL-8 (9.9-fold), MMP-9 (6.9-fold), MCP-1 (3.3-fold), Cox-2 (2.5-fold), and IκBα (2.2-fold) (Table S1). Increased expression of MMP-9, IL-8, and MCP-1 was more than additive following simultaneous TNFα stimulation and LZAP knockdown.

LZAP Is Found on Selective NF-κB-Responsive Promoters

Our data suggest that LZAP binds to RelA and inhibits transcription without altering subcellular localization of RelA. To determine if LZAP is within a DNA-associated complex at NF-κB-responsive promoter sites, we performed chromatin immunoprecipitation (ChIP) interrogating promoters of genes responsive to LZAP (MCP-1 and IL-8), as well as one gene that responded to TNFα, but not LZAP (cIAP-2). Following expression, LZAP was found associated with the NF-κB-responsive elements of MCP-1

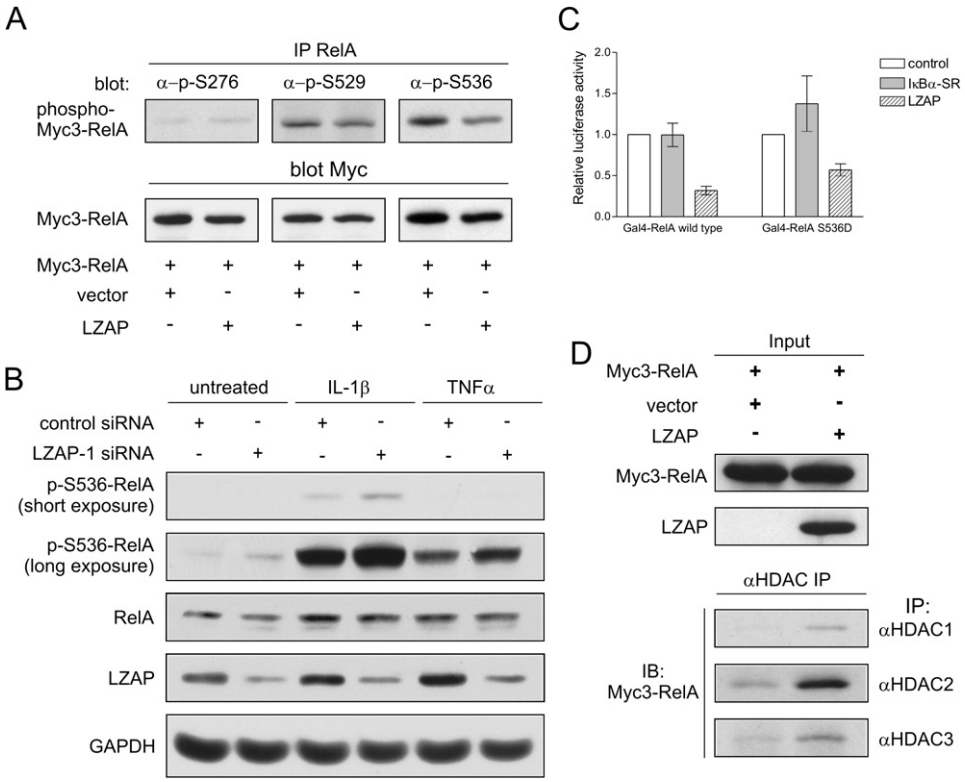

Figure 6. LZAP Regulates RelA Phosphorylation and HDAC Binding

(A) LZAP inhibits phosphorylation at serine 536 of RelA. U2OS cells were transfected with plasmids encoding Myc3-tagged RelA with or without LZAP. After TNFα treatment, RelA protein was immunoprecipitated using mouse antibody (F6), and phosphorylated Myc3-tagged RelA was visualized by immunoblotting with rabbit phosphospecific antibodies as indicated. The same membrane was stripped and reblotted with rabbit anti-RelA antibody (C20). Exposure for visualization of serine 276-phosphorylated RelA was significantly longer relative to phosphoserine 529 or phosphoserine 536.

(B) Depletion of LZAP increases phosphorylation at serine 536 of endogenous RelA. Endogenous RelA phosphorylated at serine 536 was visualized by immunoblotting lysate prepared from U2OS cells left unstimulated or cells stimulated by TNFα or IL-1β following siRNA transfection. Total RelA was immunoblotted after phosphoserine 536 RelA immunoblotting and stripping the membrane. LZAP and GAPDH were also immunoblotted.

(C) Mutation at serine 536 impairs LZAP inhibition of RelA-mediated transcription. U2OS cells were transfected with DNA constructs encoding Gal4-fused wild-type RelA or RelA S536D mutant in the absence or presence of LZAP or IκBα-SR. Luciferase expression from a Gal4-dependent reporter was determined.

(D) LZAP enhances RelA association with HDACs. U2OS cells were simultaneously transfected with control or LZAP-encoding plasmid and plasmid encoding Myc3-tagged RelA as indicated. Immunoprecipitates were prepared with goat antibodies against HDAC1, HDAC2, or HDAC3, and immunoblotted with mouse anti-RelA antibody (F6).

and IL-8 promoters, but not the cIAP-2 promoter (Figure 7A). LZAP presence at IL-8 and MCP-1 promoters was inhibited by coexpression of IκB-SR, suggesting that LZAP association with these promoter sites was dependent on NF-κB (Figure 7B). To determine if LZAP expression altered histone acetylation at NF-κB-responsive promoter elements, ChIP using anti-acetyl histone 3 antibodies was performed. LZAP expression was associated with decreased histone 3 acetylation at MCP-1 and IL-8 promoters, but not at the cIAP-2 promoter (Figure 7C).

LZAP Levels in Primary HNSCC Correlate with Expression of IL-8 and IκBα

To determine if NF-κB-responsive gene expression differed between HNSCCs dependent on LZAP expression, IL-8, IκBα, and MMP-9 expression was measured by qRT-PCR from tumors analyzed in Figure 1A. Gene expression was compared among the three groups of HNSCCs with different LZAP protein levels: (1) similar LZAP expression compared to NAT (similar, n = 16); (2) trace LZAP expression (trace, n = 4); and (3) undetectable LZAP expression (undetectable, n = 5) (Figure 8). Data were normalized to assign median expression in NAT as 1. Compared to the group of HNSCCs with LZAP protein levels similar to NAT, HNSCCs with undetectable LZAP protein contained significantly higher expression of both IL-8 and IκBα, and the group of HNSCC with low but detectable LZAP (trace) also had higher IL-8 expression (Figure 8). MMP-9 was elevated in all HNSCC groups compared to NAT but was not significantly different between the HNSCC groups based on LZAP expression. Comparison of IL-8, IκBα, and MMP-9 expression with LZAP protein levels measured within individual HNSCCs revealed that decreasing LZAP protein levels significantly correlated with increased

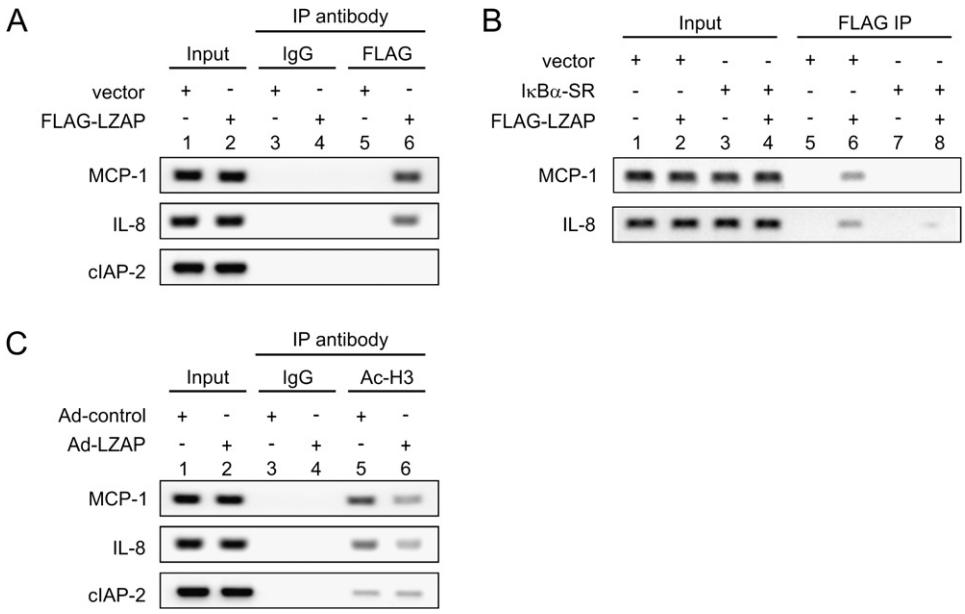

Figure 7. LZAP Binds to Specific NF-κB Target Promoters

(A) LZAP binds to NF-κB target DNA. U2OS cells were transfected with empty vector or plasmid encoding FLAG-tagged LZAP. After crosslinking, LZAP was precipitated by a mouse anti-FLAG antibody, and associated NF-κB-targeted promoter regions of MCP-1, IL-8, and cIAP-2 were detected by PCR.

(B) LZAP binding to NF-κB target DNA is inhibited by IκBα-SR. U2OS cells were transfected with empty vector or plasmids encoding FLAG-tagged LZAP with or without IκBα-SR. LZAP binding to the NF-κB-targeted promoter regions of MCP-1 and IL-8 were determined as described above.

(C) LZAP is associated with reduced histone acetylation of specific NF-κB-responsive promoters. U2OS cells were infected with control adenovirus or adenovirus expressing LZAP. ChIP analyses for indicated promoters were performed using antibody against histone 3 acetylated at lysine residues 9 and 14.

IL-8 expression (Spearman correlation test, $p = 0.001$) and also correlated with elevated IκBα expression ($p = 0.0139$). However, MMP-9 expression did not correlate with LZAP protein levels in HNSCC ($p = 0.30$).

DISCUSSION

The NF-κB family of transcription factors regulates expression of a wide range of genes that are implicated in many normal and protective biological processes, but is also usurped during tumorigenesis. Related to cancer, NF-κB regulates critical processes including apoptosis, angiogenesis, invasion, metastasis, growth, and proliferation (Hayden and Ghosh, 2004; Kim et al., 2006). NF-κB activity is tightly controlled through multiple mechanisms. Classically, NF-κB is activated by nuclear translocation triggered by phosphorylation-dependent degradation of the IκB proteins. Once in the nucleus, NF-κB binds to κB response elements and initiates transcription. A variety of nuclear proteins, including p53, ARF, Twist, Smad3, and Foxj1 regulate the strength, timing, and specificity of NF-κB activity, as well as define crosstalk with other signaling pathways (reviewed in Chen, 2004). Unlike IκB proteins that sequester NF-κB in the cytoplasm, nuclear regulators work primarily through modification of NF-κB proteins and by altering association of NF-κB with transcriptional coregulators.

Recently, the activity of NF-κB as a transcriptional repressor has also been recognized. In fact, conversion of NF-κB to an active transcriptional repressor has been reported as a mechanism through which the tumor suppressor ARF inhibits NF-κB. ARF expression results in inhibitory phosphorylation at threonine 505 of RelA mediated by the ATR-Chk1 pathway and increases association of RelA with the transcription corepressor HDAC1 without altering its DNA binding, thereby converting DNA-bound NF-κB into a potential active transcriptional repressor complex (Rocha et al., 2003, 2005). Additionally, Smad3, p53, or chemotherapeutic agents, such as cisplatin, daunorubicin, and doxorubicin, selectively alter transcriptional coregulators within NF-κB complexes, resulting in NF-κB-mediated transcriptional repression. These observations suggest that DNA-bound NF-κB complexes can be utilized to inhibit transcription under certain circumstance and that active repression contributes to overall NF-κB regulation. Although we have not formally excluded the possibility that LZAP may alter RelA sequence-specific DNA binding, LZAP was found at the promoters of NF-κB-responsive genes whose expression was altered by LZAP, and these promoters had decreased acetylation of histone 3 after LZAP expression. Additionally, expression of LZAP inhibited RelA transcription activity even in the presence of cytokine-stimulated RelA nuclear translocation and DNA binding (Figure 4, Figure 7, and Figure S1).

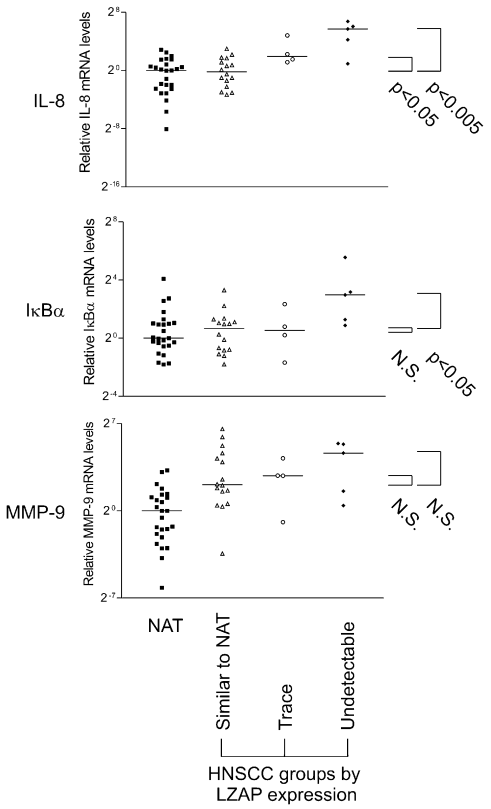

Figure 8. Loss of LZAP Protein Is Associated with Increased mRNA Levels of NF-κB-Responsive Genes

Total RNA was extracted from 25 pairs of HNSCC tumors and normal surrounding epithelia identical to those described in Figure 1A. Expression of IL-8, IκBα, and MMP-9 was determined by SYBR green-based quantitative real-time PCR using derived cDNA and corrected for input based on GAPDH expression. Data represent expression values of each gene relative to the median of expression in normal epithelia adjacent to tumor (NAT) (assigned as 1). Bars represented the median of each data set. HNSCCs were divided into three groups based on LZAP expression as described previously. The Mann-Whitney test was used to compare differences in expression of NF-κB-responsive genes between HNSCCs with trace or undetectable LZAP expression and HNSCCs with LZAP expression similar to NAT.

These data, combined with our observations that expression of LZAP resulted in decreased phosphorylation of RelA serine 536 and increased association of RelA with HDACs (Figure 6), suggest that RelA-containing NF-κB complexes act as a transcription repressor, at least toward certain NF-κB-responsive genes, in the presence of LZAP. Depletion of endogenous LZAP increased NF-κB transcription, suggesting a release of repression as indicated by both increased NF-κB-mediated transcription in reporter assays and upregulated expression of endogenous NF-κB-responsive genes such as MMP-9, IL-8, and IκBα (Figure 2 and Table S1). LZAP directly binds amino acids 195–350 of RelA by both in vivo and in vitro assays (Figure 5). Within the LZAP interacting domain of RelA is the dimerization domain, IκB-binding domain, nuclear localization signal (NLS), and several known amino acid residues involved in regulation of RelA activity. These regulatory sites include phosphor-acceptor sites, serine residues 276 and 311, and acetyl-acceptor sites, lysine residues 221 and 310. Modification of these sites has been implicated in regulation of NF-κB, and potential effects of LZAP on these modification sites are currently being explored.

Previous reports show that LZAP activates p53, resulting in cell cycle arrest and inhibition of clonogenic cell growth (Wang et al., 2006), and that LZAP increases apoptosis in response to etoposide through inappropriate stimulation of CDK1/cyclin B activity (Jiang et al., 2005). Here we ascribe other tumor suppressor-like activities to LZAP, including suppression of cellular invasion, anchorage-independent growth, tumor growth, and angiogenesis. Our data show that LZAP protein was significantly reduced in 32% of head and neck squamous cell carcinomas. As a surrogate marker for NF-κB activity, expression of three NF-κB-responsive genes was measured in these tumors. Increased expression of two genes, IL-8 and IκBα, correlated with reduced LZAP expression in HNSCC tumors ($p < 0.05$). NF-κB activity is increased in HNSCC and can be regulated at multiple levels (Chang and Van Waes, 2005; Chung et al., 2006). Correlation of LZAP levels with expression of NF-κB-regulated genes implies that LZAP may be an important regulator of NF-κB activity in primary HNSCC.

Our data suggest that LZAP is a potent regulator of basal and stimulated NF-κB activity and that loss of LZAP promotes cellular activities associated with cancer development. These data also support a role for LZAP in tumorigenesis of human HNSCC and suggest that loss of LZAP may contribute to increased NF-κB activity in HNSCC. Additional studies in other tumor types, by evaluation for mechanisms of LZAP inactivation and creation of a murine knockout model, will be necessary to confirm tumor suppressor activities of LZAP and to determine regulators of LZAP levels or activity.

EXPERIMENTAL PROCEDURES

Plasmid Constructs

Luciferase reporters, 3κB-conA-luc, and conA-luc were generous gifts from Dr. Neil Perkins (University of Dundee, Dundee, UK). Coding sequences of RelA or RelA truncation mutants were amplified by PCR and subcloned into the BamHI and XhoI sites of the pcDNA3-Myc3 expression vector, RelA and RelA S536D mutant were subcloned into the BamHI and KpnI sites of pFA-CMV vector (Stratagene, La Jolla, CA), p50 was subcloned into the EcoRI and XhoI sites of the pcDNA3-Myc3 expression vector, and LZAP coding sequence was subcloned into the KpnI and XbaI sites of the pET-His vector or the KpnI and NotI sites of the pcDNA3-FLAG vector. Other DNA constructs were described previously (Wang et al., 2006).

Antibodies and Reagents

Antibodies include mouse anti-RelA antibody F6, rabbit anti-RelA antibody C20, rabbit anti-p50 antibody H119, goat anti-HDAC1 antibody C19, goat anti-HDAC2 antibody C19, goat anti-HDAC3 antibody N19, and rabbit anti-GAPDH antibody FL335, all from Santa Cruz Biotechnology (Santa Cruz, CA); rabbit anti-phospho-S276 and -S536 RelA from Cell Signaling (Danvers, MA); rabbit anti-phospho-S529 RelA from Biosource (Carlsbad, CA); mouse anti-FLAG antibody M2 from

Sigma (St. Louis, MO); LZAP antibody has been previously described (Wang et al., 2006). TNFα and IL-1β were purchased from PeproTech (Rocky Hill, NJ).

Cell Culture, Transfection, and Retroviral Infection

Mammalian tumor cell lines were maintained at 37°C with 5% CO_2, in Dulbecco's modified Eagle's medium (DMEM) with 10% fetal bovine serum (FBS) (Invitrogen, Carlsbad, CA). Human mammary epithelial cells (TLM-HMEC), provided by Dr. William Hahn (Harvard University, Cambridge, MA), were maintained in complete mammary epithelial cell medium (MEGM, Cambrex, Baltimore, MD). Plasmids were transfected by FuGene6 (Roche, Indianapolis, IN). The total amount of transfected DNA in any single experiment was kept constant by adding empty vector (pcDNA3). Small interfering RNA (siRNA) was transfected at 20 nM by DharmaFECT 1 (Dharmacon, Chicago, IL). Control siRNA duplex (nontargeting #1) was purchased from Dharmacon. The LZAP-1 siRNA, 5′-AAGGATTGGCAGGAGATTATA (sense strand), was synthesized by QIAGEN and LZAP-2 siRNA with on-TARGETplus modification, 5′-CAAGGTATGTGGACCGAGT (sense strand), was purchased from Dharmacon. Retrovirus interfering LZAP expression was constructed by inserting LZAP-1 siRNA sequence into the HindIII and BglII sites of pRetro-Super retroviral vector (provided by Dr. Reuven Agami). Immunoprecipitation, indirect immunofluorescence, and luciferase assays have been previously described (Wang et al., 2006).

Human Tumor Studies

Human head and neck squamous cell carcinomas were collected after patient consent under an IRB-approved protocol (Head and neck tumor tissue repository and clinical database, IRB #030062). Tumors were flash frozen in liquid nitrogen within 30 min of excision and stored at −80°C until used.

Anchorage-Independent Growth Assay

TLM-HMEC cells (human mammary epithelial, stable expression of hTERT and SV40 large T antigen, and elevated expression of endogenous c-Myc) were infected with retrovirus expressing either control shRNA or LZAP-specific shRNA, and selected with 4 μg/ml puromycin. Cells (3×10^4) were seeded into 6-well plates with a bottom layer of 0.8% low-melting-temperature agar (SeaPlaque, Cambrex) in DMEM and a top layer of 0.4% agar in MEGM. Colonies with greater than 50 μm diameter were scored after 2 weeks of growth.

In Vivo Tumorigenicity Assay

Female nude mice were purchased from Harlan (Indianapolis, IN). Animals were inoculated between 8 and 16 weeks of age. HeLa cells were infected by control retrovirus or retrovirus expressing LZAP-specific shRNA, selected with puromycin, harvested, and resuspended in PBS, and 1.5×10^6 cells were injected subcutaneously into both flanks. Tumor diameter was measured weekly using calipers until the largest tumors approached 15 mm. All procedures were performed in accordance with an IACUC-approved protocol (IACUC# M/05/048). Excised tumors were weighed, then portions were frozen in liquid nitrogen or fixed in 4% paraformaldehyde before embedding in paraffin. Hematoxylin and eosin staining and immunostaining of von Willebrand Factor (vWF) were performed by the Vanderbilt Immunohistochemistry Core Laboratory. Density of blood vessels of xenograft tumors was evaluated by two independent observers (magnification = 400×). Any stained endothelial cell or endothelial cell cluster that was clearly separate from other stained endothelial cells was considered as a single, countable vessel. At least eight high-powered fields were counted for each tumor.

In Vitro Migration and Invasion Assays

Cell migration/invasion assays were performed using 24-well transwells (8 μm pore size, Corning Life Sciences), coated with (invasion) or without (migration) 60 μl 1 mg/ml matrigel (BD Sciences). U2OS cells were starved in serum-free media overnight, trypsinized, and washed three times in DMEM containing 1% FBS. Twenty thousand cells in 1% FBS-DMEM were seeded into the upper chamber, and 600 μl DMEM containing 10% or 1% FBS was placed in the lower chamber. After 16 hr incubation, matrigel and cells remaining in the upper chamber were removed. Cells on the lower surface of the membrane were fixed in 4% paraformaldehyde and stained with 0.5% crystal violet. Cells in at least six random microscopic fields (200× magnification) were counted. All experiments were run in duplicate and were repeated three times.

Zymography

Conditioned media were collected from U2OS cells after overnight culture in serum-free media. Following one freeze and thaw cycle, 10 μl conditioned media of each sample was separated on 10% standard polyacrylamide gel containing 0.1% gelatin under nonreducing conditions. After electrophoresis, gels were washed twice for 15 min in 2.5% Triton X-100, then incubated for 12 hr in developing buffer (0.5 M Tris-Hcl [pH 7.5], 10 mM $CaCl_2$). Each gel was stained with 0.5% Coomassie brilliant blue R-250 for 2 hr and destained in 50% methanol-10% acetic acid.

In Vitro Protein-Binding Assay

In vitro transcription/translation (IVT) was performed in the presences of ^{35}S-labeled methionine using TNT Quick Coupled Transcription/Translation Systems (Promega, Madison WI). His6-tagged LZAP was produced in bacteria and purified by Ni-NTA resin (QIAGEN, Valencia, CA). IVT products were equally incubated with excessive amount of His6-tagged LZAP bound to Ni-NTA resin or Ni-NTA resin only for 2 hr at room temperature with gentle agitation. Precipitates were washed with binding buffer (50 mM Tris [pH 8.0], 150 mM NaCl, 0.1% NP-40), and protein complexes associated with Ni-NTA resin were separated on SDS-PAGE and visualized by autoradiography.

ChIP

ChIP assays were performed using the chromatin immunoprecipitation assay kit (Upstate Biotechnology) according to the manufacturer's instructions. The primers used to amplify MCP-1 promoter were 5′-CCCATTTGCTCATTTGGTCTCAGC and 5′-GCTGCTGTC TCTGCCTCTTATTGA, and the primers used to amplify IL-8 and cIAP-2 promoter were previously described (Ashburner et al., 2001; Hoberg et al., 2004).

Supplemental Data

The Supplemental Data include Supplemental Experimental Procedures, two supplemental figures, and one supplemental table and can be found with this article online at http://www.cancercell.org/cgi/content/full/12/3/239/DC1/.

ACKNOWLEDGMENTS

We thank Neil Perkins, William Hahn, and Reuven Agami for reagents and Robbert Slebos for statistical assistance. We are extremely grateful to Neil Perkins, Jennifer Pietenpol, and Robbert Slebos for insightful advice. Support for this research was provided by grant #2R01 DE013173-05 from the National Institute of Dental and Craniofacial Research to W.G.Y.; by an endowment in support of the Barry Baker Laboratory for Head and Neck Oncology at Vanderbilt; by the Vanderbilt-Ingram Cancer Center and the Robert J. and Helen C. Kleberg Foundation; and by grants from the National Institute of Allergy and Infectious Disease (#AI35098), the National Cancer Institute (#CA73756 and #CA75080 to A.S.B.), and the National Cancer Institute (#CA104397 and #CA095644 to M.W.M.). Support to W.G.Y. is provided through an Ingram Professorship of Cancer Research. A.S.B. is an investigator of the Waxman Cancer Research Foundation.

Received: December 14, 2006
Revised: April 26, 2007
Accepted: July 6, 2007
Published: September 10, 2007

REFERENCES

Ahuja, D., Saenz-Robles, M.T., and Pipas, J.M. (2005). SV40 large T antigen targets multiple cellular pathways to elicit cellular transformation. Oncogene *24*, 7729–7745.

Ashburner, B.P., Westerheide, S.D., and Baldwin, A.S., Jr. (2001). The p65 (RelA) subunit of NF-κB interacts with the histone deacetylase (HDAC) corepressors HDAC1 and HDAC2 to negatively regulate gene expression. Mol. Cell. Biol. *21*, 7065–7077.

Bond, M., Fabunmi, R.P., Baker, A., and Newby, A.C. (1998). Synergistic upregulation of metalloproteinase-9 by growth factors and inflammatory cytokines: An absolute requirement for transcription factor NF-κB. FEBS Lett. *435*, 29–34.

Chang, A.A., and Van Waes, C. (2005). Nuclear factor-κB as a common target and activator of oncogenes in head and neck squamous cell carcinoma. Adv. Otorhinolaryngol. *62*, 92–102.

Chen, F. (2004). Endogenous inhibitors of nuclear factor-κB, an opportunity for cancer control. Cancer Res. *64*, 8135–8138.

Chen, L.F., and Greene, W.C. (2004). Shaping the nuclear action of NF-κB. Nat. Rev. Mol. Cell Biol. *5*, 392–401.

Chung, C.H., Parker, J.S., Ely, K., Carter, J., Yi, Y., Murphy, B.A., Ang, K.K., El-Naggar, A.K., Zanation, A.M., Cmelak, A.J., et al. (2006). Gene expression profiles identify epithelial-to-mesenchymal transition and activation of nuclear factor-κB signaling as characteristics of a high-risk head and neck squamous cell carcinoma. Cancer Res. *66*, 8210–8218.

Fingleton, B. (2006). Matrix metalloproteinases: Roles in cancer and metastasis. Front. Biosci. *11*, 479–491.

Hayden, M.S., and Ghosh, S. (2004). Signaling to NF-κB. Genes Dev. *18*, 2195–2224.

He, C. (1996). Molecular mechanism of transcriptional activation of human gelatinase B by proximal promoter. Cancer Lett. *106*, 185–191.

Hoberg, J.E., Yeung, F., and Mayo, M.W. (2004). SMRT derepression by the IκB kinase α: A prerequisite to NF-κB transcription and survival. Mol. Cell *16*, 245–255.

Jiang, H., Luo, S., and Li, H. (2005). Cdk5 activator-binding protein C53 regulates apoptosis induced by genotoxic stress via modulating the G2/M DNA damage checkpoint. J. Biol. Chem. *280*, 20651–20659.

Karin, M., Cao, Y., Greten, F.R., and Li, Z.W. (2002). NF-κB in cancer: From innocent bystander to major culprit. Nat. Rev. Cancer *2*, 301–310.

Kim, H., and Koh, G. (2000). Lipopolysaccharide activates matrix metalloproteinase-2 in endothelial cells through an NF-κB-dependent pathway. Biochem. Biophys. Res. Commun. *269*, 401–405.

Kim, H.J., Hawke, N., and Baldwin, A.S. (2006). NF-κB and IKK as therapeutic targets in cancer. Cell Death Differ. *13*, 738–747.

Liu, X., Yuan, H., Fu, B., Disbrow, G.L., Apolinario, T., Tomaic, V., Kelley, M.L., Baker, C.C., Huibregtse, J., and Schlegel, R. (2005). The E6AP ubiquitin ligase is required for transactivation of the hTERT promoter by the human papillomavirus E6 oncoprotein. J. Biol. Chem. *280*, 10807–10816.

Magal, S.S., Jackman, A., Ish-Shalom, S., Botzer, L.E., Gonen, P., Schlegel, R., and Sherman, L. (2005). Downregulation of Bax mRNA expression and protein stability by the E6 protein of human papillomavirus 16. J. Gen. Virol. *86*, 611–621.

Mantovani, F., and Banks, L. (2001). The human papillomavirus E6 protein and its contribution to malignant progression. Oncogene *20*, 7874–7887.

Perkins, N.D. (2004). Regulation of NF-κB by atypical activators and tumour suppressors. Biochem. Soc. Trans. *32*, 936–939.

Rocha, S., Campbell, K.J., and Perkins, N.D. (2003). p53- and Mdm2-independent repression of NF-κB transactivation by the ARF tumor suppressor. Mol. Cell *12*, 15–25.

Rocha, S., Garrett, M.D., Campbell, K.J., Schumm, K., and Perkins, N.D. (2005). Regulation of NF-κB and p53 through activation of ATR and Chk1 by the ARF tumour suppressor. EMBO J. *24*, 1157–1169.

Takada, Y., Andreeff, M., and Aggarwal, B.B. (2005). Indole-3-carbinol suppresses NF-κB and IκBα kinase activation, causing inhibition of expression of NF-κB-regulated antiapoptotic and metastatic gene products and enhancement of apoptosis in myeloid and leukemia cells. Blood *106*, 641–649.

Viatour, P., Merville, M.P., Bours, V., and Chariot, A. (2005). Phosphorylation of NF-κB and IκB proteins: Implications in cancer and inflammation. Trends Biochem. Sci. *30*, 43–52.

Wang, C.Y., Mayo, M.W., and Baldwin, A.S., Jr. (1996). TNF- and cancer therapy-induced apoptosis: Potentiation by inhibition of NF-κB. Science *274*, 784–787.

Wang, J., He, X., Luo, Y., and Yarbrough, W.G. (2006). A novel ARF-binding protein (LZAP) alters ARF regulation of HDM2. Biochem. J. *393*, 489–501.

Westbrook, T.F., Martin, E.S., Schlabach, M.R., Leng, Y., Liang, A.C., Feng, B., Zhao, J.J., Roberts, T.M., Mandel, G., Hannon, G.J., et al. (2005). A genetic screen for candidate tumor suppressors identifies REST. Cell *121*, 837–848.

Ying, H., and Xiao, Z.X. (2006). Targeting retinoblastoma protein for degradation by proteasomes. Cell Cycle *5*, 506–508.

Zhang, Y., Xiong, Y., and Yarbrough, W.G. (1998). ARF promotes MDM2 degradation and stabilizes p53: ARF-INK4a locus deletion impairs both the Rb and p53 tumor suppression pathways. Cell *92*, 725–734.